THE ROLE OF MAGNETIC RESONANCE CEREBROSPINAL FLUID FLOWMETRY IN THE CLINICAL FIELD

By

Moataz Abou-Zeid Mohamed Abou-Zeid*, Mohamed Farouk Aggag*, Mohamed Salah El-Feshawy* and Mahmoud Galal Ahmed**

Department of Diagnostic & Interventional Radiology* and Neurology**, Faculty of Medicine, Al-Azhar University

Corresponding Author: Moataz Abou-Zeid Mohamed Abou-Zeid,

Mobile: +201016536565, **E-mail:** docmoatazabozeid@gmail.com

ABSTRACT

Background: MRI Phase contrast (PC MRI) CSF flowmetry is a reliable noninvasive method used multiple different parameters to detect the CSF motion through aqueduct of sylvius.

Objective: To evaluate the role of MRI phase contrast CSF flowmetry in diagnosis of CSF motion in various brain pathologies.

Patients and methods: Fifty patients were in this study. This study was performed between August 2020 and May 2021, at Department of Diagnostic and Interventional Radiology, Al-Azhar University Hospitals in Cairo. Patients were referred from Neurology Department and outpatients MRI radiology unit at Al-Hussein University Hospital in Cairo. In our study we used 6 parameters including the Peak of the mean diastolic and systolic velocities in cm/sec, (PDV and PSV), Maximum velocity (Vmax) in cm/sec, ROI area which is aqueduct area measured in cm2. Maximum flow in cm3/sec. and the usual CSF volume passing within the aqueduct during systole and diastole which is called Stroke volume and measured in µl/cycle. We used PC MRI to assess the connection between the subarachnoid spaces and the arachnoid cyst, which benefits in treatment selection. patients with hydrocephalus by PC MRI that illustrated the sort of hydrocephalus and the reason for obstruction in non-communicating type.

Results: CSF flow indices were higher than ordinary in normal pressure hydrocephalus (NPH) and idiopathic intracranial hypertension (IIH) while in brain atrophy (BA) the CSF flow indices were lower than typical. In Chiari malformation type I (CM-I) patients we applied PC MRI method at the aqueduct level and cranio cervical junction (CCJ) level. The velocities were fundamentally higher than typical in CM-I at aqueduct level. However, non-high at the degree at CCJ level, through the endoscopic third ventriculostomy (ETV) stoma. CSF flow by PC MRI and tracked down that high stroke volume (SV) was a good index for successful ETV.

Conclusion: MRI CSF flowmetry gave simple, precise and noninvasive technique for analysis and follow up of various diseases of neurology that interfered with normal CSF flow. Also, it tended to be direction for legitimate treatment choice.

Keywords: CSF flowmetry, PC MRI, CSF pathology.

INTRODUCTION

Phase contrast MRI (PC MRI) CSF flowmetry the most important indicator in diagnosis and to follow up IIH patients *(Akay et al., 2015)*. Also, to discriminate among normal pressure hydrocephalus and brain atrophy use PC MRI. The most important indicator in diagnosis and to

follow up IIH patients is PC MRI is arising (MRI) technique tends to be utilized for the qualitative and quantitative evaluation of CSF motion at key anatomic locations, like the cerebral aqueduct of Sylvius and the foramen magnum *(Alves et al., 2017)*. For differentiation among communicative and non-communicative hydrocephalus, shows whether if there is any communication between arachnoid cysts and the subarachnoid space or not, show the CSF flow irregularity that outcomes from Chiari 1 malformation owing to tonsillar herniation *(Bladowska and Sąsiadek, 2018)*. PC MRI after Endoscopic third ventriculostomy (ETV) can explain an accurate technique to follow up of effective flow through the stoma *(Hassanien et al., 2018)*. To discriminate among normal pressure hydrocephalus and brain atrophy use PC MRI. The most important indicator in diagnosis and to follow up IIH patients is PC MRI.

The present work aimed to evaluate the role of MRI phase contrast CSF flowmetry in diagnosis of CSF motion in various brain pathologies.

PATIENTS AND METHODS

This was prospective study including a total of 50 patients (25 males and 25 females) with their ages ranged from 1 to 70 years with mean age of 40.82±15.20 years, during the period between August 2020 and May 2021, at Department of Diagnostic and Interventional Radiology, Al-Hussein University Hospital in Cairo. Agreement of the ethical committee, and written informed permissions from all the patients were obtained.

Inclusion criteria:

- Patients at any age from 1 to 70 years and of both sexes.

- The patients in our study were divided into:

  - Control group Subjects were free from any medical or neurological disease and had standard conventional MRI.

  - Idiopathic intracranial hypertension group based on clinical symptoms, ophthalmology examination and high CSF pressure on lumbar puncture.

  - Normal pressure hydrocephalus group with Symptoms of Hakim triad (gait disturbance, dementia and urine incontinence).

  - Brain atrophy group overlapping symptoms with NPH Patients.

  - Chiari type I malformation group referred by common complaint of headache aggravated by straining. They were diagnosed by tonsillar herniation below the foramen magnum in Conventional MRI.

  - Endoscopic third ventriculostomy group who underwent ETV and came for follow up.

  - Arachnoid cyst group referred from Neurology Department by headache. They were diagnosed to have intracranial arachnoid cyst by conventional MRI.

  - Hydrocephalus group referred from Neurology Department by variable symptoms (headache, nausea and gait unsteadiness). All were diagnosed by conventional

MRI by having signs of hydrocephalus (Evan index>0.3 and narrowed cortical sulci).

Exclusion criteria

These criteria were set to ensure patient safety and avoidance of complications, these criteria were patients who had:

- A cardiac pacemaker.

- A metallic foreign body in their eye.

- An aneurysm clip in their brain.

- Any electrically or magnetically activated implants (cochlear implants).

- Patients with severe claustrophobia.

- Uncooperative patients with excessive motion.

- Bad general condition.

Phase contrast MRI Protocol:

1.5 T magnetic resonance scanner (Philips Achieva, Netherland).

For sagittal 2D phase contrast image the following parameters were used:

- TR 21 ms.

- TE ranged from 5.4 to 10 ms.

- Flip angle 10°.

- Matrix 256x256 pixels.

- Slice thickness=5mm.

For axial phase contrast image, the following parameters were used:

- TR ranged from 12 to 17 ms.

- TE ranged from 7.3 to 10.4 ms.

- Flip angle=15°.

- Matrix 256x256 pixels.

- Slice thickness=5mm.

Velocity encoding (VENC) was adjusted for each category, in standard CSF flow imaging the VENC value is 5–8 cm/sec. for arachnoid cysts and brain atrophy Lower VENC range (2–4 cm/sec). NPH and through the stoma of ETV patients higher VENC range (20–25 cm/sec). In midsagittal image a localizer was located at right angles to the aqueduct of sylvius, the localizer should go through the aqueduct in the axial plane. Phase contrast images were obtained in one heart cycle. A series of phase and magnitude images at various heart phases were attained. A similar strategy was applied to the craniocervical junction (CCJ) and endoscopic third ventriculostomy (ETV) stoma. For arachnoid cyst valuation, the plane of imaging is changed according to the predictable site of connection to the subarachnoid space which may be in axial, coronal or sagittal planes. After the records achievement all images were conveyed to the workstation equipment with Q flow software. The CSF flow indices were mechanically extracted afterward a region of interest (ROI) was lined out by hand to cover all pixels that revealed the CSF flow signals on the phase images after amplification of the images to explain the flow.

Qualitative analysis was done in midsagittal phase and magnitude images which showed the CSF flow in systole and diastole, the hyperintense signal represents (caudal flow) in systole, while the hypointense signal represented the (cranial flow) in diastole, the change in flow in the ETV stoma, aqueduct and CCJ during systole and diastole to preclude the presence of obstruction. For arachnoid cyst, evaluation of connection with the subarachnoid CSF space was done

through searching for pulsatile CSF flow (alteration of hypo and hyperintense signal) in phase images in the suitable plane of imaging at the neck of the cyst, absence of such a signal ruled out the communication.

Quantitative analysis:

- Peak systolic (PSV) and diastolic (PDV) velocities: were obtained from the mean velocity-time curve. In this curve the area above the baseline represented the diastolic flow with its furthermost point is the peak diastolic velocity in cm/sec, the area under the baseline represented the systolic velocity with the furthermost point from the baseline represented the peak systolic velocity which is measured in cm/sec unit.

- (Vmax) Maximum velocity was measured by (PSV + PDV) divided by 2

- The region of interest (ROI) which represented the aqueduct area and measured by (cm2).

- To calculate the maximum flow, we used the following formula (maximum flow equals Maximum velocity X aqueduct area).

- The mean volume of CSF passed through the region of interest (ROI) area in one heart cycle was calculated by adding forward and backward flow and dividing the result by two which is called The Stroke volume.

Analytical statistics: Statistical analysis of the data: Data were tabulated, coded then analyzed using the computer program SPSS (Statistical package for social

science) version 17.0 to obtain descriptive statistics were calculated in the form of:

1. Mean ±Standard deviation (SD).

2. Median and range (minimum-maximum).

3. Frequency (number-percent).

In the statistical comparison between the different groups, the significance of difference was tested using one of the following tests:

1. Student's t-test (Unpaired): Used to compare between mean of two different groups of numerical (parametric) data.

2. Mann Whitney test: Used to compare between two different groups of numerical (non-parametric) data.

3. Repeated measures ANOVA (analysis of variance) test: Used to compare between more than two related groups of numerical (parametric) data followed by post-hoc Bonferroni.

4. Friedman test: Used to compare between more than two related groups of numerical (non-parametric) data followed by pairwise comparisons.

5. Inter-group comparison of categorical data was performed by using Fisher's-exact test.

A P value <0.05 was considered statistically significant.

RESULTS

The outcome of the disease in each age group was variable **(Table 1)**.

Table (1): Age differences in each disease category

Age / Differences	Mean	±SD	Median	Minimum	Maximum
Aqueduct control category	25.67	7.79	23	13	45
CCJ control category	38.33	12.57	32	28	55
IIH category	24.29	7.21	26	8	40
NPH category	51.73	7.26	53	38	70
BA category	54.5	2.87	55	48	63
CM-I category	27.5	7.88	24	20	42
ETV category	13.5	12.73	14	6	30
Arachnoid cyst category	5.5	10.4	6	1	19
Hydrocephalus category	29.8	19.9	35.5	5.5	54

The outcome of the disease in each sex group was variable **(Table 2).**

Table (2): Gender differences in each disease category

Sex / Differences	Male No	Male %	Female No	Female %	Total No	Total %
Aqueduct control category	2	40.00%	3	60.00%	5	100%
CCJ control category	2	66.67%	1	33.33%	3	100%
IIH category	0	0.00%	8	100.00%	8	100%
NPH category	8	61.54%	5	38.46%	13	100%
BA category	4	57.14%	3	42.86%	7	100%
CM-I category	1	33.33%	2	66.67%	3	100%
ETV category	2	66.67%	1	33.33%	3	100%
Arachnoid cyst category	1	33.33%	2	66.67%	3	100%
Hydrocephalus category	5	100.00%	0	0.00%	5	100%

The highest PSV and SV were found in NPH patients **(Table 3)**.

Table (3): Phase contrast parameters for aqueduct control category, IIH category, NPH category and BA category collectively

Categories / Parameters	Aqueduct control category (n=5) Mean	±SD	IIH category (n=8) Mean	±SD	NPH category (n=13) Mean	±SD	BA category (n=7) Mean	±SD
PDV(cm/sec)	2.10	0.38	3.55	0.96	4.25	1.17	1.34	0.45
PSV(cm/sec)	2.75	0.60	4.18	1.16	4.95	1.60	1.68	0.56
Vmax (cm/sec)	2.45	0.28	3.80	0.97	4.57	1.29	1.48	0.45
SV (µl/cycle)	25.34	5.35	39.27	16.48	83.22	27.50	11.64	4.32
Aqueduct area (cm2)	0.047	0.014	0.050	0.017	0.077	0.029	0.049	0.011
Maximum flow (cm3/sec)	0.117	0.044	0.186	0.065	0.349	0.133	0.073	0.025

All the PC MRI parameters showed significant increase in NPH patients compared to the control group as shown in **Table (4)**.

Table (4): Control category versus NPH category

Parameters \ Categories	Aqueduct control category (n=5)		NPH category (n=13)		P
	Mean	±SD	Mean	±SD	
PDV(cm/sec)	2.10	0.38	4.25	1.17	<0.002
PSV(cm/sec)	2.75	0.60	4.95	1.60	<0.003
Vmax(cm/sec)	2.45	0.28	4.57	1.29	<0.0011
SV (µl/cycle)	25.34	5.35	83.22	27.50	<0.005
Aqueduct area (cm^2)	0.047	0.014	0.077	0.029	0.007
Maximum flow (cm^3/sec)	0.117	0.044	0.349	0.133	<0.006
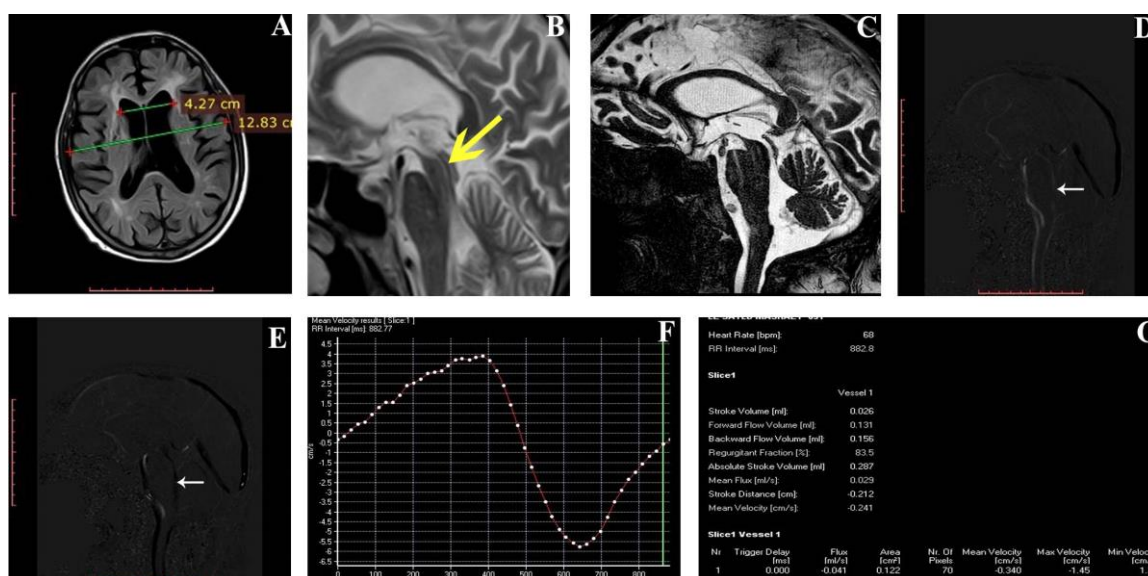
Figure (1): Case 1. Male patient aged 69 years old complained of urinary incontinence, memory disturbance and gait apraxia.

a) Axial FLAIR MRI at the level of the lateral ventricle showing hydrocephalus (Evan index=0.33).
b) Sagittal T2 WI MRI showing marked low at the aqueduct (signal void sign).
c) patent normal aqueduct so excluding obstruction in 3D DRIVE image.
d) In systole, the CSF flow in the aqueduct of sylvius appears as shades of white in Sagittal phase image.
e) In diastole the CSF flow in the aqueduct of sylvius appears as shades of black, so confirm absence of obstruction in sagittal phase image.
f) According to the curve showing CSF in both systole (below the base line) and diastole (above the base line), peak systolic velocity=5.8 cm/sec, peak diastolic velocity =3.9 cm/sec. maximum velocity =(3.9+5.8) / 2 = 4.85 cm/sec.
g) CSF flow curve table signifying:
   • backward flow volume=156 µl, Forward flow volume= 131 µl and so the stroke volume = (131+156) / 2 =143.5 µl/cycle.
   • Aqueduct surface area=0.122 cm^2. So, the maximum flow = 4.85 X 0.122 = 0.5917 cm^3/sec.

Diagnosis: NPH with Hyperdynamic CSF circulation.

All the PC MRI parameters showed significant decrease in BA patients compared to the control group as shown in **Table (5)**.

Table (5): Control category versus BA category

Categories / Parameters	Aqueduct control category (n=5)		BA category (n=7)		P
	Mean	±SD	Mean	±SD	
PDV(cm/sec)	2.10	0.38	1.34	0.45	0.002
PSV(cm/sec)	2.75	0.60	1.68	0.56	0.003
Vmax(cm/sec)	2.45	0.28	1.48	0.45	<0.004
SV (µl/cycle)	25.34	5.35	11.64	4.32	<0.005
Aqueduct area (cm^2)	0.047	0.014	0.049	0.011	0.98
Maximum flow (cm^3/sec)	0.117	0.044	0.073	0.025	0.016
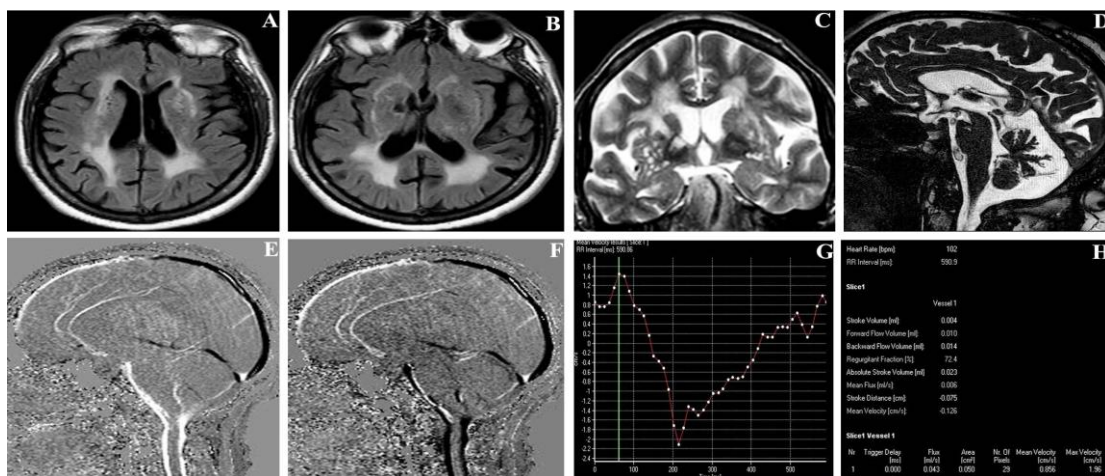
Figure (2): Case 2. Patient 68 years old of male gender presented by challenging urinary control, mentality impairment and gait disturbance

A & B) MRI Axial FLAIR images showing mild dilatation of the lateral ventricles, abnormal hyperintensity in white matter representing ischemic changes and prominent subarachnoid space and cortical sulci.

C) Coronal T2 WI showing prominent subarachnoid space and cortical sulci and dilated Virchow Robin spaces.

D) patent normal aqueduct so excluding obstruction in 3D DRIVE image.

E) In systole, the CSF flow in the aqueduct of sylvius appears as shades of white in Sagittal phase image.

F) in diastole the CSF flow in the aqueduct of sylvius appears as shades of black in Sagittal phase image, so confirm absence of obstruction.

G) According to the curve showing CSF in both systole (below the base line) and diastole (above the base line) peak diastolic velocity = 1.42 cm/sec, peak systolic velocity = 2.22 cm/sec. maximum velocity =(1.42+2.22) / 2 = 1.82 cm/sec.

H) CSF flow curve table signifying:

- Backward flow volume=14 µl, forward flow volume= 10 µl and so the stroke volume = (10+14) / 2 =12 µl/cycle.
- Aqueduct surface area=0.05 cm^2. So, the maximum flow = 1.8 X 0.05 = 0.09 cm^3/sec.

Diagnosis: brain atrophy with Hypodynamic CSF flow.

All the PC MRI parameters showed significant increase in IIH patients compared to the control group as shown in **Table (6)**.

Table (6): Control category against IIH category

Categories \ Parameters	Aqueduct control category (n=5)		IIH category (n=8)		P
	Mean	±SD	Mean	±SD	
PDV(cm/sec)	2.10	0.38	3.55	0.96	0.003
PSV(cm/sec)	2.75	0.60	4.18	1.16	0.004
Vmax(cm/sec)	2.45	0.28	3.80	0.97	0.001
SV (µl/cycle)	25.34	5.35	39.27	16.48	0.006
Aqueduct area (cm^2)	0.047	0.014	0.050	0.017	0.7
Maximum flow (cm^3/sec)	0.117	0.044	0.186	0.065	0.004
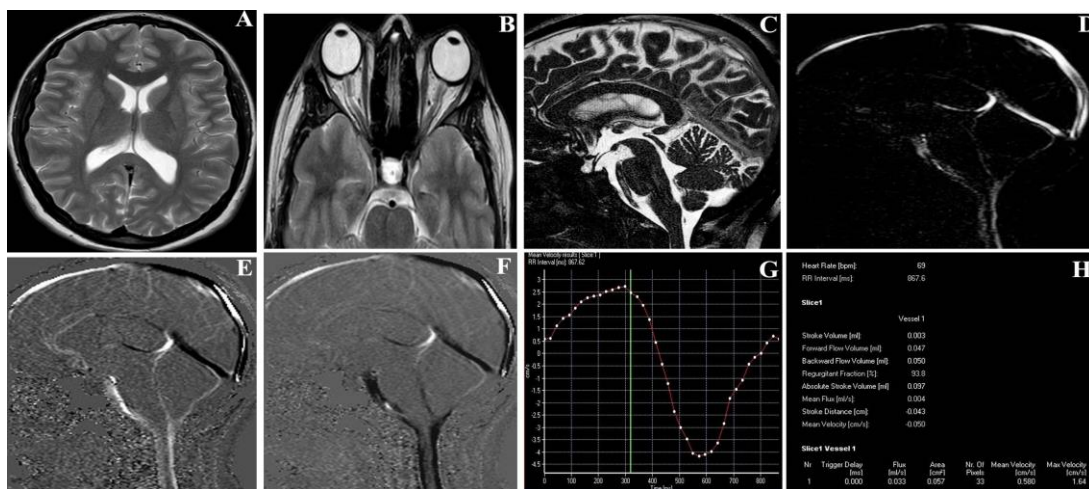
Figure (3): Case 3 patient aged 38 years old of female gender complaining of visual impairment and headache. The fundus examination revealed papilledema. Also, the CSF opening pressure was high

a) MRI Axial T2 WI showing no dilatation of the lateral ventricles.

b) MRI Axial T2 WI at the level of eye globe showing kinking of both orbital nerves and widening of the perioptic CSF space. Also note the partial empty sella.

c) Patent normal aqueduct so excluding obstruction in 3D DRIVE image.

d) The CSF flow in the aqueduct of sylvius appears as shades of white (Regardless of the direction of flow) in Sagittal Magnitude image.

e) In systole, the CSF flow in the aqueduct of sylvius appears as shades of white in Sagittal phase image in.

f) In diastole the CSF flow in the aqueduct of sylvius appears as shades of black in sagittal phase image, so confirm absence of obstruction.

g) According to the curve showing CSF in both systole (below the base line) and diastole (above the base line). peak diastolic velocity = 2.6 cm/sec, peak systolic velocity = 4.18 cm/sec. maximum velocity =(2.6+4.18) / 2 = 3.39 cm/sec.

h) CSF flow curve table signifying:
- Backward flow volume=50 µl and Forward flow volume= 47 µl so the stroke volume = (47+50) / 2 =48.5 µl/cycle.
- Aqueduct surface area=0.057 cm^2. So, the maximum flow was calculated as following: maximum flow= 3.35 X 0.057 = 0.19059 cm^3/sec.

Diagnosis: IIH with Hyperdynamic CSF circulation.

The PSV and PDV parameters exhibited significant increase in CM- I group compared to the control group. Whereas, the SV parameter revealed a non-significance pattern as shown in **Table (7)**.

Table (7): Aqueduct control category versus CM-I category

Categories / Parameters	Aqueduct control category (n=5)		CM-I category (n=3)		P
	Mean	±SD	Mean	±SD	
Aqueduct PDV(cm/sec)	2.10	0.38	3.96	2.25	0.029
Aqueduct PSV(cm/sec)	2.75	0.60	4.95	1.68	0.004
Aqueduct SV (µl/cycle)	25.34	5.35	37.39	16.22	0.07

PC MRI parameters used at the CCJ level were PSV and PDV. They were extracted for each compartment distinctly. This was applied for both CM-I group and new control group at the CCJ and results were summarized as shown in **Table (8)**.

Table (8): CCJ control category versus CM-I category

Categories / Parameters	CCJ control category (n=3)		CM-I category (n=3)		P
	Mean	±SD	Mean	±SD	
CCJ anterior compartment PDV(cm/sec)	1.46	0.14	2.29	0.85	0.17
CCJ anterior compartment PSV(cm/sec)	1.75	0.43	3.68	1.88	0.16
CCJ posterior compartment PDV(cm/sec)	0.84	0.13	1.08	0.25	0.18
CCJ posterior compartment PSV(cm/sec)	1.28	0.16	1.33	0.38	0.9
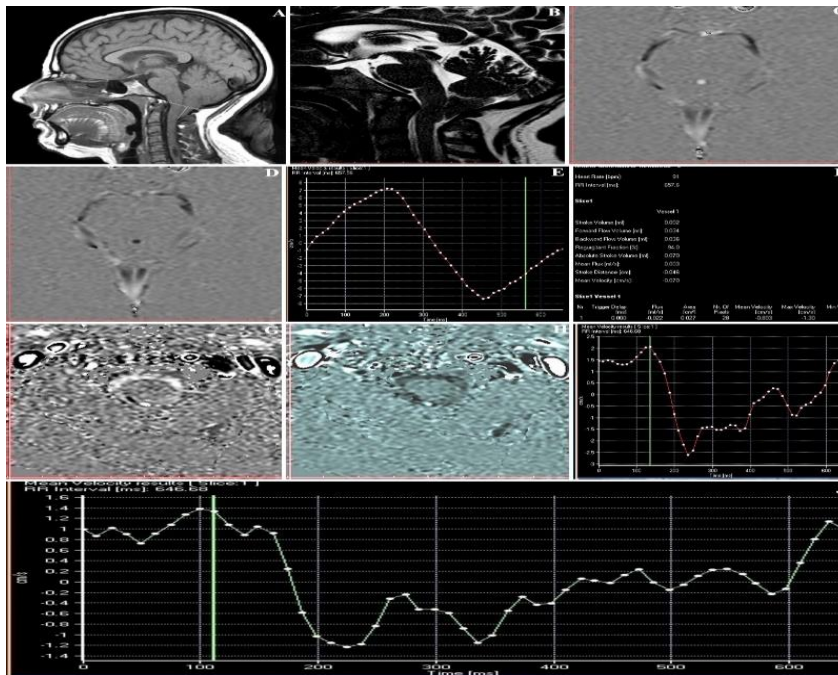
Figure (4): Case 4 patient aged 30 years old of female gender presented with headache that become worsened with straining. Patient underwent conventional MR imaging and phase contrast MRI at 2 levels: Aqueduct level and craniocervical junction (CCJ) level

a) MRI Sagittal T1 WI showing cerebellar tonsil herniates under the foramen magnum by 24 mm. Also, Syrinx is seen within the spinal cord opposite C5-6.
b) Patent aqueduct with flow void sign indicating high velocity in 3D DRIVE image.
c) In systole, the CSF flow in the aqueduct of Sylvius as shades of white at axial phase image.
d) In diastole, the CSF flow in the aqueduct of Sylvius appears as shades of black at axial phase image.
e) According to the curve at the level of the aqueduct showing CSF in both systole (below the base line) and diastole (above the base line). Peak diastolic velocity = 7.2 cm/sec, peak systolic velocity = 7.4 cm/sec.
f) CSF flow curve table demonstrating:
   • Backward flow volume=36 µl, Forward flow volume= 34 µl and so the Stroke volume = (34+36) / 2 =35 µl/cycle.
g) The CCJ in systole showing CSF flow as shades of white in axial phase image.
h) The CCJ in diastole showing CSF flow as shades of black in axial phase image.
i) Curve of velocity time at anterior compartment showing CSF in both systole (below the base line) and diastole (above the base line) . peak diastolic velocity = 2.1 cm/sec, peak systolic velocity = 2.7 cm/sec.
j) Curve of velocity time at posterior compartment showing CSF in both systole (below the base line) and diastole (above the base line). peak diastolic velocity = 1.4 cm/sec, peak systolic velocity = 1.2 cm/sec.
o) Note that the curve become more irregular posteriorly.

Diagnosis: Chiari malformation type I associated with cord syrinx causing CSF flow abnormality which was reflected at the CCJ.
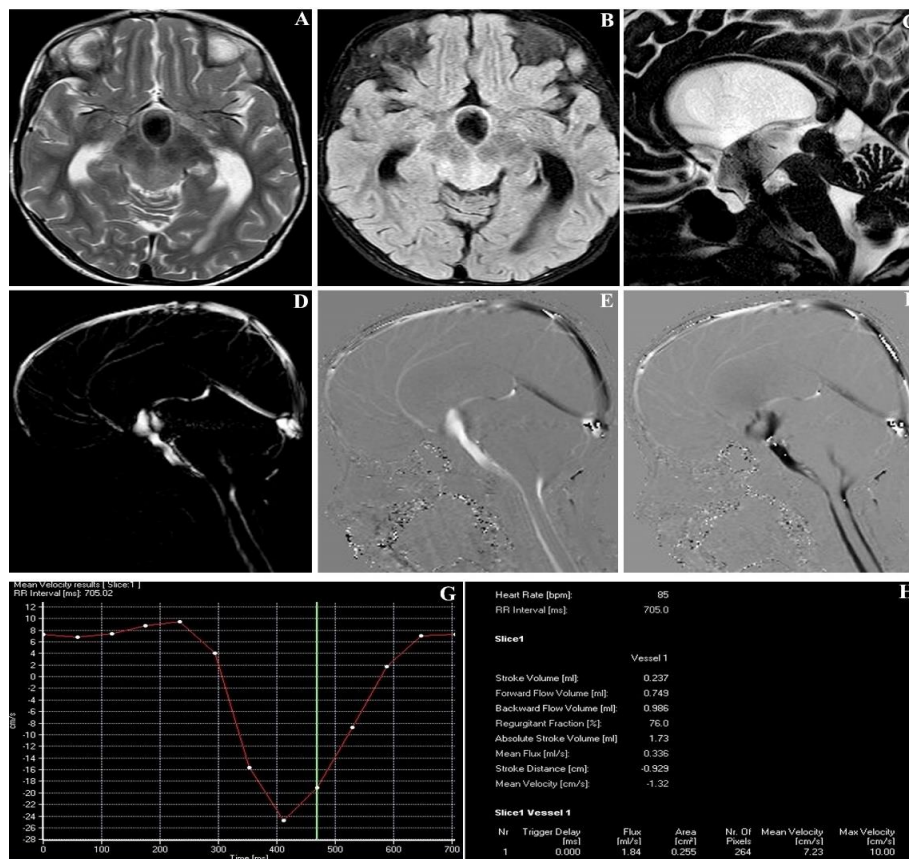
Figure (5): Case 5. Female patient aged 7 years old "diagnosed as obstructive hydrocephalus caused by tectal glioma" underwent (ETV) endoscopic third ventriculostomy and came for follow up with good postoperative clinical outcome

a) MRI Axial T2 WI shows the marked low signal of CSF flow through the ETV stoma (signal void sign), also note the tectal glioma.

b) MRI Axial FLAIR image showing the signal void CSF flow through the ETV stoma, Also the tectal glioma is seen.

c) Obstructed aqueduct by tectal glioma and showing the flow void sign through the ETV stoma, 3rd ventricle and the prepontine cistern (grade III) in 3D DRIVE image.

d) Sagittal magnitude image showing CSF flow through the ETV stoma between the prepontine cistern and the 3rd ventricle as shades of white regardless the direction of flow.

e) in systole showing CSF flow through the ETV stoma between the between the prepontine cistern and the 3rd ventricle as shades of white in sagittal phase image.

f) In diastole showing CSF flow as shades of black in sagittal phase image.

g) Curve of velocity time showing CSF in both systole (below the base line) and diastole (above the base line). Peak diastolic velocity = 10 cm/sec, peak systolic velocity = 25 cm/sec.

h) CSF flow curve table demonstrating:
   - Backward flow volume=996 µl, Forward flow volume= 749 µl and the stroke volume= 872 µl/cycle.
   - The area of ETV stoma =0.255 cm^2.

Diagnosis: Opened ETV stoma with high SV.
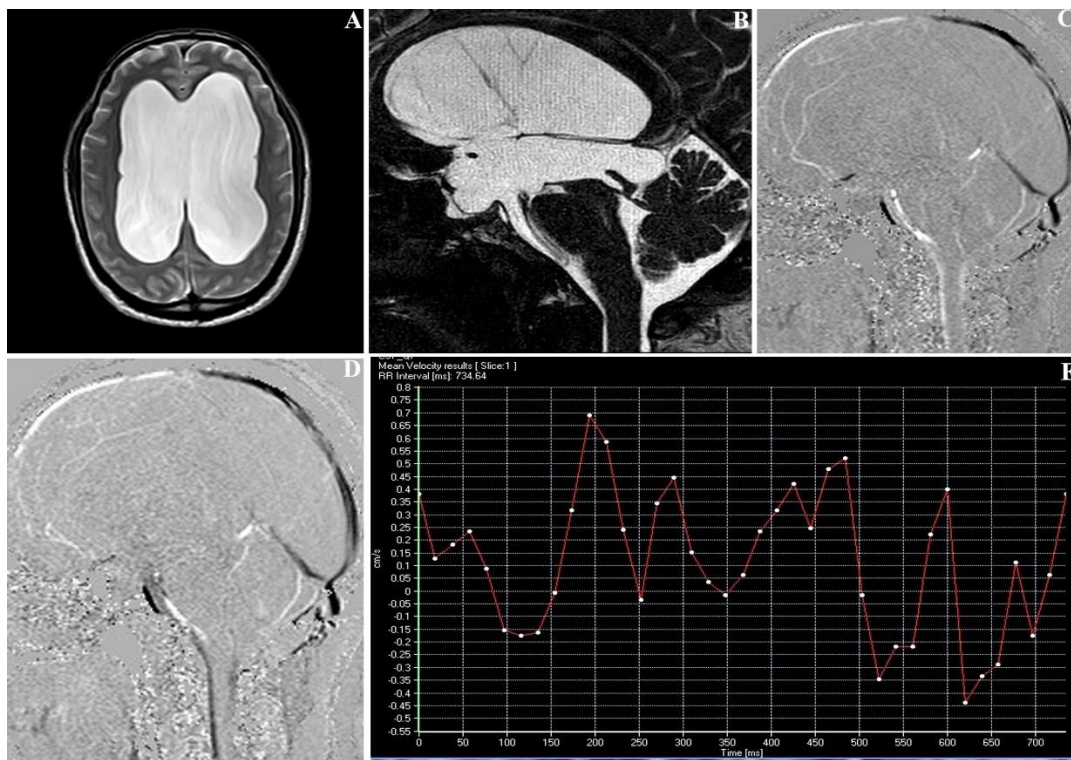
Figure (6): Case 6. patient aged 46 years old of male gender presented by visual impairment, headache and gait disturbances

a) MRI Axial T2 WI showing hydrocephalus.
b) Aqueductal web in 3D DRIVE image.
c) In systole showing absent CSF flow in the aqueduct at sagittal phase image.
d) In diastole showing absent CSF flow in the aqueduct at sagittal phase image.
e) Curve of velocity time showing significantly irregular CSF flow curve indicating irregular to and fro motion of the CSF proximal to the location of obstruction.

Diagnosis: Aqueductal web causes obstructive hydrocephalus.
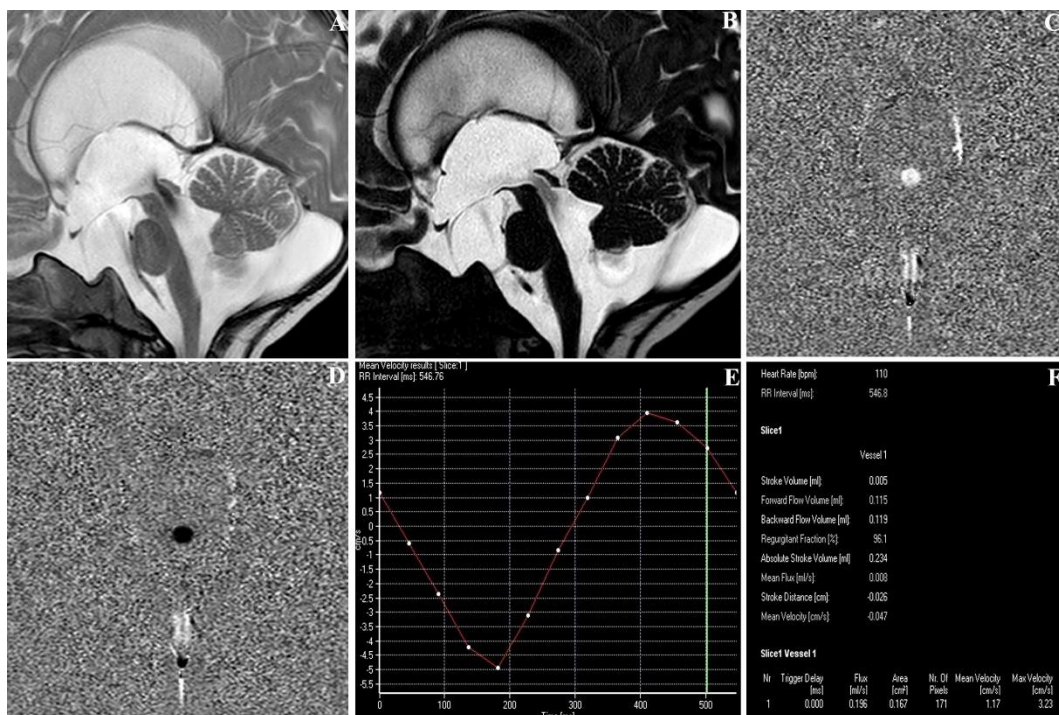
Figure (7): Case 7. patient aged 1 year old of male gender presented with progressive increase in size of the head and delayed milestones

a) MRI Mid-sagittal T2 WI showing tetra-ventricular dilatation and flow void sign at the aqueduct.

b) Patent normal aqueduct with flow void sign, so excluding obstruction in 3D DRIVE image.

c) In systole, the CSF flow in the aqueduct of sylvius appears as shades of white at axial phase image.

d) In diastole the CSF flow in the aqueduct of sylvius appears as shades of black, so confirm absence of obstruction at axial phase image.

e) Curve of velocity time showing CSF in both systole (below the base line) and diastole (above the base line). Peak diastolic velocity= 4 cm/sec, peak systolic velocity = 5 cm/sec.

f) CSF flow curve table demonstrating:

• Backward flow volume=119 µl, forward flow volume= 115 µl and so the stroke volume =117 µl/cycle.

Diagnosis: communicating hydrocephalus with hyper dynamic CSF circulation.

MOATAZ M. ABOU-ZEID *et al.,*
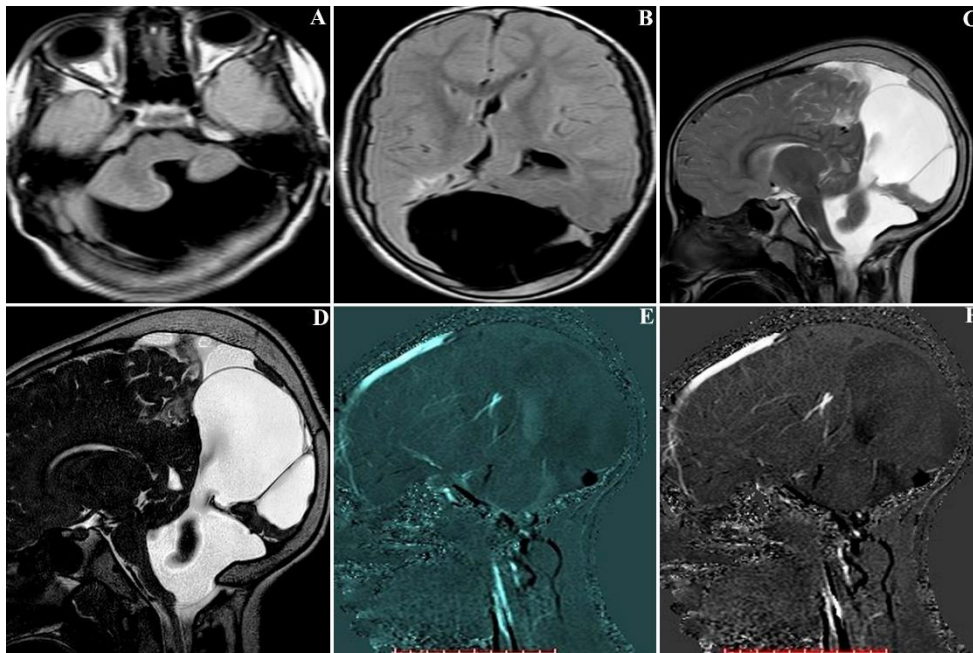
Figure (8): Case 8. Female patient aged 12 years diagnosed as Dandy Walker malformation associated with inter-hemispheric cyst

a) MRI Axial FLAIR image showing absent cerebellar vermis and presence of retrocerebellar cyst connected to the 4th ventricle.
b) MRI Axial FLAIR image showing posterior interhemespheric cyst.
c) MRI Sagittal T2 WI shows both cysts in the same image.
d) Showing the two cysts in the same view, the inter-hemispheric cyst is multilocular with possible communication with the retrocerebellar cyst at 3D DRIVE image.
e) In systole showing pulsatile CSF flow at the neck of the retro-cerebellar cyst as well as inter-hemispheric cyst as shades of white at sagittal phase image.
f) In diastole showing pulsatile CSF flow at the neck of the retro-cerebellar cyst as well as inter-hemispheric cyst as shades of black at sagittal phase image.

Diagnosis: The retro-cerebellar cyst was connected to the 4th ventricle. The inter-hemispheric cyst had a communication with the retro-cerebellar one.

Figure (9): Case 9. Male patient aged 23 years presented with cerebellar manifestation

a) Sagittal T2 WI shows retro-cerebellar arachnoid cyst with tetra-ventricular dilatation more marked at the 4th ventricle.
b) Retro-cerebellar arachnoid cyst with tetra-ventricular dilatation more marked at the 4th ventricle. Note the fine septa within the 4th ventricle at 3D DRIVE image.
c) In systole showing **no** pulsatile CSF flow at the neck of the retro-cerebellar cyst at sagittal phase image.
d) In diastole showing **no** pulsatile CSF flow at the neck of the retro-cerebellar cyst at sagittal phase image.

Diagnosis: The retro-cerebellar cyst was non communicating cyst.

DISCUSSION

In our study, we used 6 parameters including the PSV and PDV which were measured in cm/sec; maximum velocity (Vmax) in cm/sec. Aqueduct surface area was represented by the region of interest (ROI) area and measured in cm2. Maximum flow in cm3/sec, and the average of the CSF volume passing through aqueduct during systole and diastole was stroke volume which was measured in µl/cycle. While *Akay et al., (2015)* utilized aqueduct area, peak rate,

mean rate, mean flow, forward flow volume and backward flow volume.One of the few treatable causes of dementia is normal pressure hydrocephalus. NPH patients after ventriculo-peritoneal shunt show great improvement of clinical symptoms. Symptoms of NPH are not unique for it and also it is difficult to accurately discriminate it from brain atrophy *(Liu and Digre, 2013)*.

In our study, we utilized PC MRI at the level of aqueduct of sylvius in 13 patients with normal pressure hydrocephalus. There was a critical increase in all indices utilized in NPH category contrasted with control category representing CSF flow hyperdynamic in patients of NPH. The all parameters utilized in brain atrophy were found to be significantly reduced than the control category demonstrating CSF flow of hypodynamic nature. Idiopathic intracranial hypertension was diagnosed by elevated intracranial pressure without any obvious reason. We applied PC MRI with the same six indices on 8 patients with clinically suspected IIH referred from neurology department and we discovered a significant increase in all indices. These outcomes were in equivalent with *Akay et al. (2015)*.

In Chiari malformation, regarding CSF flow between spinal subarachnoid space and the intracranial there was increased resistance, we can aid clinicians to select patients who need surgical intervention and follow up them postoperatively by Recognition of the severity of such CSF flow irregularity *(Dlouhy et al., 2017)*.

We examined 3 Chiari malformation type I patients by PC MRI at 2 levels, at the craniocervical junction and at the aqueduct of sylvius. We utilized (PSV)

Peak systolic velocity, (PDV) Peak diastolic velocity and (SV)stroke volume at the aqueduct of sylvius. After comparing the results of CM-I category with our control category, we discovered significant increase in Peak systolic velocity (PSV) and Peak diastolic velocity (PDV) in CM-I patients by comparison to the control category. Anyway, the SV index showed non significance. This was in agreement with *Wang et al. (2014)* who discovered significant increase in Peak systolic velocity (PSV) and Peak diastolic velocity (PDV) in CM-I patients comparative to the healthy control group.

As regard the craniocervical junction level, we studied CSF flow changes in both the ventral and the dorsal regions of the CCJ around the spinal cord by PC MRI using peak velocity parameters only (PSV and PDV). Then we applied the same technique for new control group (CCJ control group). We compared the results of CM-I group with that of the control group at the CCJ level. This revealed that all the PC MRI parameters used showed non significance in comparison with the control group in both ventral and dorsal compartments.

One of the most progressively utilized these days rather than shunt operation in selected cases of obstructive hydrocephalus is Endoscopic third ventriculostomy (ETV). Evaluation of effective ETV dependent on clinical base or conventional MRI is not precise since the clinical improvement might be slow and influenced by different issues. PC MRI can be utilized to quantify the flow of CSF at the ETV stoma *(Alves et al. 2017)*. In our research, we examined 3 patients who undertook ETV and came for

follow up by PC MRI utilizing the following indices: PSV, PDV, SV and ROI area. All patients displayed high velocities and stroke volume and this was in match with the respectable clinical outcome in all the three patients. This was in agreement with *Dinçer et al. (2011)* who found that the stroke volume at ETV stoma is a good pointer of the functional status of ETV, and a high stroke volume seems to be a positive indicator of great clinical results. So, PC MRI gave precise technique to guarantee patency and good function of the ETV stoma after operation.

Arachnoid cysts may or may not have a connection with the subarachnoid space which thus influences appropriate treatment choice for symptomatic patients. Such a communication may be noticed by invasive examinations such as ventriculography, CT cisternography (CTC) and MR cisternography (MRC). PC MRI offers a noninvasive technique to verify or deny existence of such a communication *(Li et al., 2013)*. We have the arachnoid cysts disease in three patients. Two of them were identified as communicating cysts on base of recognition of pulsatile CSF flow at the neck of the cyst as (black and white signal alteration). Just one case was identified as non-communicating cyst because of absence of such a signal.

Hydrocephalus is a vague diagnosis that may outcome from many variable causes. Communicating and non-communicating (obstructive) hydrocephalus are the main two types of hydrocephalus. The reason for hydrocephalus might be evident by conventional MRI. But if the reason is questionable, phase contrast MRI can be utilized to distinguish between non-communicating and communicating hydrocephalus *(Bladowska and Sąsiadek, 2018)*. In our study, 5 patients identified to have hydrocephalus by conventional MRI were further explored utilizing PC MRI, which discovered the reason for hydrocephalus precisely. One patient was identified as communicating hydrocephalus (had no obstructive cause at the level of ventricular system by 3D-DRIVE, and was confirmed by quantification of CSF flow that shown hyperdynamic CSF flow). The aqueductal CSF flow velocity to be essentially higher in communicating hydrocephalus patients than normal volunteers. The rest 4 cases were identified as obstructive hydrocephalus by combination of ordinary MRI, 3D DRIVE and quantitative analysis through the aqueduct (revealed irregular CSF flow curve). This was harmonious with *Lucic et al. (2012)* who studied PC MRI in patients with aqueductal pathology and discovered the curve to be asymmetrical in cases of obstruction. Also, *Bladowska and Sąsiadek (2018)* stated that sagittal heavily T2-weighted DRIVE are compulsory sequence in the accurate assessment of obstructive hydrocephalus.

CONCLUSION

The most noninvasive, easy and precise technique for diagnosis and follow up of various neurological diseases that interfere with normal CSF flow also, it can be guidance for accurate treatment decision is phase contrast cerebrospinal fluid (CSF) flowmetry MRI.

REFERENCES

1. **Akay R., Kamisli O., Kahraman A., Oner S. and Tecellioglu M. (2015):** Evaluation of aqueductal CSF flow dynamics with phase contrast cine MR imaging in idiopathic intracranial hypertension patients: preliminary results. Eur Rev Med Pharmacol Sci 19, 3475-9.

2. **Alves T., Ibrahim E.-S., Martin B and Malyarenko D (2017):** Principles, techniques, and clinical applications of phase-contrast magnetic resonance cerebrospinal fluid imaging. Neurographics, 7: 199-210.

3. **Bladowska J. and Sąsiadek M.J. (2018):** Obstructive Hydrocephalus in Adults. In: Clinical Neuroradiology: The ESNR Textbook (eds. by Barkhof F, Jager R, Thurnher M & Rovira Cañellas A). PP: 1-23. Pbl.Springer International Publishing, Cham..

4. **Dinçer A., Yildiz E., Kohan S. and Özek M.M. (2011):** Analysis of endoscopic third ventriculostomy patency by MRI: value of different pulse sequences, the sequence parameters, and the imaging planes for investigation of flow void. Child's Nervous System, 27: 127-35.

5. **Dlouhy B.J., Dawson J.D. and Menezes A.H. (2017):** Intradural pathology and pathophysiology associated with Chiari I malformation in children and adults with and without syringomyelia. Journal of Neurosurgery: Pediatrics, 20: 526-41.

6. **Hassanien O.A., Abo-Dewan K.A., Mahrous O.M. and El Kheshin S.E. (2018):** Evaluation of the patency of endoscopic third ventriculostomy using phase contrast MRI-CSF flowmetry as diagnostic approach. The Egyptian Journal of Radiology, 49: 701-10.

7. **Li L., Zhang Y., Li Y., Zhai X., Zhou Y. and Liang P. (2013):** The clinical classification and treatment of middle cranial fossa arachnoid cysts in children. Clinical Neurology and Neurosurgery, 115: 411-8.

8. **Liu G.T. and Digre K.B. (2013):** Revised diagnostic criteria for the pseudotumor cerebri syndrome in adults and children. Neurology, 81: 1159-65.

9. **Lucic M., Bjelan M., Koprivsek K., Lucic S., Kozic D., Sveljo O., Spirovski M. and Kamenica S. (2012):** Quantitative dynamic phase-contrast MRI analysis of the CSF flow values within the stenotic and obstructed cerebral aqueduct. In: Euroepan Congress of Radiology, Vienna, European Society of Radiology, pp. 1-7.

10. **Wang C.-S., Wang X., Fu C.-H., Wei L.-Q., Zhou D.-Q. & Lin J.-K. (2014):** Analysis of cerebrospinal fluid flow dynamics and morphology in Chiari I malformation with cine phase-contrast magnetic resonance imaging. Acta neurochirurgica 156, 707-13.

دور الرنين المغناطيسي لقياس تدفق السائل النخاعي بالمخ في المجال الاكلينيكي

معتز أبو زيد محمد أبو زيد*، محمد فاروق عجاج*، محمد صلاح الفيشاوي*، محمود جلال أحمد**

قسم الأشعة التشخيصية والتداخلية* وقسم طب المخ والاعصاب**، كلية الطب، جامعة الأزهر، القاهرة، مصر

E-mail: docmoatazabozeid@gmail.com

خلفيـــة البحـــث: اخـــتلال تـــدفق السـائل النخـاعي يمكـن أن يكـون سـبب أو مؤشـر للأمـراض، والـرنين المغناطيسـي ذو التبـاين المرحلـي أثبـت كونـه وسـيلة معتمـدة وغير مؤذية للتقييم النوعي والكمي لتدفق السائل النخاعي.

الهـدف مـن البحـث: توضـيح قيمـة الـرنين المغناطيسـي ذو التبـاين المرحلـي فـي تشـخيص الأمـراض العصـبية المختلفة التـي تتسـبب فـي خلـل فـي تـدفق السـائل النخاعي.

المرضـي وطـرق البحـث: أجريـت هـذه الدراسـة خـلال الفتـرة مـن اغسـطس 2020م وحتـى مـايو 2021م فـي قسـم الأشـعة التشخيصـية والتداخليـة بمستشـفي الحسـين الجـامعي بالقـاهرة، وكـان عـدد المرضـى 50 مريضـاً مـن الـذين تـرددوا علـى وحـدة الـرنين المغناطيسـي بمستشـفي الحسـين الجـامعى او الـذين تـم تحـويلهم مـن قسـم طـب المـخ والاعصـاب لعمـل رنـين ذو التبـاين المرحلـى بوحـدة الـرنين المغناطيسـي بمستشـفي الحسـين الجـامعى بالقـاهرة، وكـانوا مـن أمـراض عصـبية مختلفـة: مرضـى الاستسـقاء الـدماغي ذو الضـغط الطبيعـي (13 مـريض)، والضـمور المخـي (7 مرضـى)، ومرضـى إرتفـاع ضـغط المـخ الغيـر مسـبب (8 مـريض)، ومرضـى تشـوهات كيـاري النـوع الأول (3 مرضـى)،و المرضـى الـذين خضـعوا لمنظـار لإحـداث ثقـب علاجـي فـي البطـين الثالـث للمـخ (3مرضـى)،و مرضـى لـديهم أكيـاس عنكبوتيـة (3 مرضـى)، و مرضـى الاستسـقاء الـدماغي (5 مرضـى). وقـد خضـع جمـيعهم للفحـص بـالرنين المغناطيسـي المعتـاد ثـم الـرنين المغناطيسـي ذو التبـاين المرحلي.

نتـائج البحـث: كانـت المؤشـرات المسـتخدمة لقيـاس تـدفق السـائل النخـاعي أعلـى مـن الطبيعـي فـي مرضـى الاستسـقاء الـدماغي ذو الضـغط الطبيعـي و حـالات ارتفـاع ضـغط المـخ الغيـر مسـبب. وكانـت المؤشـرات أقـل مـن الطبيعـي فـي مرضـى الضـمور المخـي. أمـا مرضـى تشـوهات كيـاري النـوع الأول، فلقـد طبقنـا تقنيـة الـرنين المغناطيسـي ذو التبـاين المرحلـي علـيهم علـى مسـتوى القنـاة الدماغيـة وعلـى مسـتوى وصلـة المـخ بالنخـاع الشـوكي. ولقـد وجـدنا أن سـرعات تـدفق السـائل النخـاعي كانـت أعلـى مـن الطبيعـي فـي حـالات تشـوهات كيـاري علـى مسـتوى القنـاة الدماغيـة، بينمـا لـم يكـن هنـاك فـارق ذو تـأثير فـي المؤشـرات علـى مسـتوى وصلـة المـخ بالنخـاع الشـوكي.لقد قمنـا بقيـاس كميـة السـائل النخـاعي المتـدفق خـلال الثقـب الـذي تـم عملـه بالمنظـار فـي البطـين الثالـث للمـخ ووجـدنا أن قيـاس حجـم السـائل النخـاعي التـي تمـر خـلال هـذا الثقـب مـع كـل نبضـة قلبيـة كـان مؤشـرا جيدا لنجـاح هـذه العمليـة. استطاع الـرنين المغناطيسـي ذو التبـاين المرحلـي فـي ايجـاد اتصـال بـين الأكيـاس العنكبوتيـة الممتلئـة بالسـائل النخـاعي الموجـودة داخـل الجمجمـة وبـين أمـاكن السـائل النخـاعي الاخـرى داخـل الجمجمـة والتـي بـدورها تحـدد طريقـة عـلاج هـذه الأكياس.واستطعنا معرفـة مرضـى الاستسـقاء الـدماغي باسـتخدام الـرنين المغناطيسـي ذو التبـاين المرحلـي وتحديـد نـوع الاستسـقاء الـدماغي (متصـل أو غيـر متصـل) وأيضاً قمنـا بإيجاد سبب الانسداد في حالات الاستسقاء الدماغي الغير متصل.

الاسـتنتاج: الـرنين المغناطيسـي لقيـاس تـدفق السـائل النخـاعي بـالمخ هـو طريقـة سـهلة ودقيقـة وغيـر مؤذيـة لتشـخيص ومتابعـة مختلـف الأمـراض العصـبية التـي تـؤدي الـى اختـلال فـي تـدفق السـائل النخـاعي بـالمخ، وأيضـا يمكـن ان تكـون مرشـدا فـي اختيـار طريقة العلاج المناسبة.

الكلمـات الدالـة: قيـاس تـدفق السـائل النخـاعى بـالمخ، الـرنين المغناطيسـي ذو التبـاين المرحلى، امراض السائل النخاعى.